Urban Europe and NSFC

Europe – China joint call on Sustainable Urbanisation in the Context of Economic Transformation and Climate Change: Sustainable and Liveable Cities and Urban Areas

Funded by
NCN (Poland), project UMO-2018/29 / Z / ST10 / 02986
NSFC (China), project 71961137011
FFG (Austria), project 870234

UNCNET

Urban nitrogen cycles: new economy thinking to master the challenges of climate change

D3/2: A quantitative estimate of the impacts of ammonia emissions on urban $PM_{2.5}$ air quality

Due date of deliverable: **31/08/2020** Actual submission date: **18/10/2020**

Start Date of Project: **01/04/2019** Duration: **35 months**

Organisation name of co-chairs for this deliverable: **PKU**

Authors: Zehui Liu, Lin Zhang

Dissemination Level		
PU	Public	☐
PP	Restricted to other programme participants (including funding agencies)	☒
RE	Restricted to a group specified by the consortium (including funding agencies)	☐
CO	Confidential, only for members of the consortium (including funding agencies)	☐

Executive Summary

The North China plain, including megacities such as Beijing and Shijiazhuang, has experienced severe fine particulate matter ($PM_{2.5}$) air pollution in recent years. To mitigate $PM_{2.5}$ air pollution, stringent emission controls have then been implemented through the Five-Year Plan and the Action Plan on Prevention and Control of Air Pollution that mainly control primary PM emissions and the emissions of aerosol precursors (SO_2 and NO_x). Ammonia (NH_3), another important precursor of secondary inorganic aerosols (SIA), also plays a critical role in $PM_{2.5}$ air pollution. NH_3 in the atmosphere first reacts with sulfuric acid (H_2SO_4 as produced from oxidation of SO_2) to form ammonium sulfate aerosol, and excessive NH_3 then reacts with nitric acid (HNO_3 as produced from oxidation of NO_2) to form ammonium nitrate aerosol. However, NH_3 emissions have not been regulated yet in China. This raises an issue that how effective NH_3 emission controls can achieve on urban $PM_{2.5}$ air quality with changing SO_2/NO_x emissions.

As part of the task of UNCNET WP3, we investigate the impacts of NH_3 emissions on $PM_{2.5}$ air pollution over Beijing-Tianjin-Hebei (BTH) region using a regional air quality model (The Weather Research and Forecasting (WRF) Version 3.6.1 model coupled with Chemistry (WRF-Chem)) combined with our recent developed Chinese agricultural NH_3 emission inventory. We conduct a series of model simulations to quantify the impacts of NH_3 emissions on urban $PM_{2.5}$ air quality under different NH_3 emission reduction conditions as well as under different SO_2 and NO_x emission conditions (e.g., considering the 2015-2017 SO_2/NO_x emission changes). Obtaining a quantitative estimate of the effectiveness of NH_3 emission reductions on $PM_{2.5}$ air pollution regulation will help policy makers to optimize emissions reduction strategies.

We find strong nonlinear responses of $PM_{2.5}$ air pollution to NH_3 emission reductions in North China. Under the current NH_3 emission condition changes in $PM_{2.5}$ concentrations in North China associated with NH_3 emission reductions follow a power exponential function in January. The BTH mean PWC $PM_{2.5}$ concentrations in January would only decrease 1.4-3.8 $\mu g\ m^{-3}$ (1.1-2.9% of $PM_{2.5}$) when NH_3 emissions in North China were reduced by 20-40%, but the decreases would reach 8.1-26.7 $\mu g\ m^{-3}$ (6.2-20.5% of $PM_{2.5}$) with 60-100% NH_3 emission reductions. Such nonlinearity reflects a switch of NH_3-saturated to NH_3-limited condition for SIA, in particular, aerosol nitrate formation. The $PM_{2.5}$ changes in July also show a nonlinear response, but the nonlinearity is much weaker than January.

As SO_2 emissions in North China have substantially reduced over 2015-2017, we find that has lowered the efficiency of NH_3 emission controls on $PM_{2.5}$ air pollution in both winter and summer. Future reductions of NO_x emissions may partly enhance $PM_{2.5}$ pollution in BTH winter due to the weakened titration effect, and can be offset by jointly controlling NH_3 emissions. Our results emphasize the importance of an accurate NH_3 emission estimate on the assessment of effectiveness of NH_3 emission controls, and also support the need to jointly consider emission reductions of SO_2, NO_x, and NH_3 for mitigating SIA air pollution in the BTH region.

ANNEX 1

The nonlinear response of fine particulate matter pollution to ammonia emission reductions in North China

Manuscript to be submitted to Environmental Research Letters
(revised version, October 2020)

The nonlinear response of fine particulate matter pollution to ammonia emission reductions in North China

Zehui Liu[1], Lin Zhang[1], Mi Zhou[1], Youfan Chen[1], Dan Chen[2], Qi Chen[3], Yuepeng Pan[4], Tao Song[4], Dongsheng Ji[4]
[1]Laboratory for Climate and Ocean-Atmosphere Studies, Department of Atmospheric and Oceanic Sciences, School of Physics, Peking University, Beijing 100871, China
[2]Institute of Urban Meteorology, Beijing, 100089, China
[3]State Key Joint Laboratory of Environmental Simulation and Pollution Control, College of Environmental Sciences and Engineering, Peking University, Beijing 100871, China
[4]State Key Laboratory of Atmospheric Boundary Layer Physics and Atmospheric Chemistry (LAPC), Institute of Atmospheric Physics, Chinese Academy of Sciences, Beijing 100029, China

Abstract
Recent Chinese air pollution actions have significantly lowered the fine particulate matter ($PM_{2.5}$) levels in North China via controlling emissions of sulfur dioxide (SO_2) and nitrogen oxides (NO_x) together with other primary aerosols, while emissions of another precursor, ammonia (NH_3) have not been regulated. This raises a question that how effective NH_3 emission controls can achieve on $PM_{2.5}$ pollution with changing SO_2/NO_x emissions. Here we use a regional air quality model to investigate this issue accounting for different NH_3 emission reductions and different SO_2/NO_x emissions in North China. We find that the $PM_{2.5}$ reduction efficiency of NH_3 emission controls is highly sensitive to the NH_3 emission condition and reduction strength. The Beijing-Tianjin-Hebei regional population weighted $PM_{2.5}$ concentrations would only decrease 1.4-3.8 μg m^{-3} (1.1-2.9% of $PM_{2.5}$) with 20-40% NH_3 emission reductions, but reach 8.1-26.7 μg m^{-3} (6.2-20.5%) with 60-100% NH_3 emission reductions in January 2015. The 2015-2017 emission changes (reduction in SO_2 emissions) have lowered the efficiency of NH_3 emission controls. NO_x emission reductions may enhance wintertime $PM_{2.5}$ pollution due to the weakened titration effect and can be offset by jointly controlling NH_3 emissions. Our results emphasize the need to jointly consider NH_3 emission controls when designing $PM_{2.5}$ pollution mitigation strategies.

Keywords
ammonia, air pollution, fine particulate matter, $PM_{2.5}$, emission reduction

Submitted to the Environmental Research Letters, ***
Revised ***

1. Introduction

Fine particulate matter (particle with aerodynamic diameters less than or equal to 2.5 μm; also referred as $PM_{2.5}$) not only poses serious harm to human health but also adversely influences atmospheric environment (Li *et al* 2014; Gao *et al* 2016; Liao *et al* 2015). The North China plain has experienced severe $PM_{2.5}$ air pollution in recent years, and drawn worldwide attention (Huang *et al* 2014; Zhang *et al* 2015). To abate $PM_{2.5}$ air pollution, the Chinese government has implemented the "Action Plan on Prevention and Control of Air Pollution" in 2013 and "Three-year Action Plan Fighting for a Blue Sky" in 2018 (Zhang *et al* 2019; Chinese State Council 2013, 2018). The annual mean $PM_{2.5}$ concentration in the Beijing-Tianjin-Hebei (BTH) region has decreased from 106 μg m^{-3} in 2013 to 64 μg m^{-3} in 2017 (MEE 2013; MEE 2017). This value is still much higher than the China's National Ambient Air Quality Standard (NAAQS) of 35 μg m^{-3}, and calls for more stringent emission control measures.

Ammonia (NH_3) is a vital alkaline gas in the ambient atmosphere and plays a critical role in nitrogen deposition and haze pollution (Pan *et al* 2018; Wang *et al* 2013; Zhang *et al* 2015). NH_3 in the air first reacts with sulfuric acid (H_2SO_4 as produced from oxidation of SO_2) to form ammonium sulfate aerosol, and excessive NH_3 then reacts with nitric acid (HNO_3 as produced from oxidation of NO_2) to form ammonium nitrate aerosol. These secondary inorganic aerosols (SIA, including sulfate, nitrate, and ammonium) account for 30-50% of $PM_{2.5}$ in the eastern China (Zhao *et al* 2013; Huang *et al* 2014; Sun *et al* 2016). Depending on the abundance of NH_3 in the air, the formation of SIA can be considered as the NH_3-poor condition (when there is no sufficient NH_3 to neutralize H_2SO_4) or the NH_3-rich condition (when there is NH_3 to further neutralize HNO_3) (Seinfeld and Pandis, 2006). When NH_3 is too abundant, formation of aerosol nitrate becomes HNO_3-limited, and most NH_3 remains gaseous in the atmosphere (Xu *et al* 2019). The availability of NH_3 also significantly modulates liquid aerosol pH and then affects the heterogenous chemistry on the aerosol surface (Ge B *et al* 2019).

Air pollution actions in China have implemented a series of emission control measures mainly targeting fuel combustion induced emissions of SO_2, NO_x ($NO+NO_2$), and other primary aerosols (Zhang *et al* 2019). NH_3 emissions are dominantly from agricultural activities (i.e., fertilizer application, livestock manure management) (Zhang *et al* 2018) and have not been regulated yet in China (Fu *et al* 2017; Zheng *et al* 2018). The recent "Three-year Action Plan Fighting for a Blue Sky" called for agricultural NH_3 emission controls but did not establish a target reduction amount (Chinese State Council, 2018). Atmospheric chemistry modelling studies indicated that controlling agricultural NH_3 emissions would significantly decrease aerosol nitrate in North China in particular during severe winter haze events (Xu *et al* 2019; Han *et al* 2020), while thermodynamic calculations suggested that a substantial (> 50%) NH_3 emission reduction was required to effectively reduce SIA levels under present winter haze conditions in this region (Guo *et al* 2018; Song *et al* 2019). The discrepancy can be largely induced by the accuracy of NH_3 emission estimates, and the effectiveness of NH_3 emission controls on $PM_{2.5}$ under the conditions of rapid SO_2 and NO_x emission changes as occurring in North China is still undetermined.

Here we investigate the issue using a regional air quality model combined with our recent developed Chinese agricultural NH_3 emission inventory (Zhang *et al* 2018). We conduct a series of model simulations to quantify the effectiveness of NH_3 emission reductions on $PM_{2.5}$ air pollution regulation under different NH_3 emission reduction conditions as well as under different SO_2 and NO_x emission conditions (e.g., considering the 2015-2017 SO_2/NO_x emission changes)

2. Methodology and data

The Weather Research and Forecasting (WRF) Version 3.6.1 model coupled with Chemistry (WRF-Chem) is employed to simulate meteorological fields and atmospheric chemistry in North China. The modeling framework is configured with two domains (Figure S1) using 161 (east-west) ×171 (south-north) and 150 (east-west) × 159 (south-north) grid cells at 27 km and 9 km horizontal resolutions, respectively. The outer domain covers China and its adjacent areas, and the inner domain covers North China where this study focuses on. The National Center for Environmental Prediction (NCEP) Final (FNL) Analysis data with 1-degree spatial resolution and 6-hour temporal resolution are used for the initial and lateral boundary conditions of meteorology in the model. The meteorological fields are re-initiated every two days using the FNL Analysis data so that they are nearly the same for all our simulations. The chemical initial and boundary conditions are obtained from the outputs of the global chemical transport model MOZART-4 (Emmons *et al* 2010).

Our simulations use the gas-phase Carbon-Bond Mechanism Z (CBMZ) mechanism (Zaveri and Peters, 1999) coupled with a 4-bin sectional (0.039-0.156, 0.156-0.625, 0.625-2.5, and 2.5-10.0 μm for dry diameter) Model for Simulating Aerosol Interactions and Chemistry (MOSAIC) aerosol scheme (Zaveri *et al* 2008). We have implemented the heterogeneous sulfate formation reactions on particle surface based on Chen *et al* (2016) to improve the model simulation of secondary inorganic aerosols, and have increased the anthropogenic OC emissions by a factor of 4 to account for secondary organic aerosols in the model (Sun *et al* 2012). The new gas-particle partitioning module Adaptive Step Time-Split Euler Method (ASTEM) is used to determine the NH_3 and HNO_3 gas-aerosol equilibrium (Zaveri *et al* 2008).

The model physical settings include the Morrison double-moment microphysics scheme (Morrison *et al* 2009), the Grell-3 cumulus scheme (Grell *et al* 2002), the RRTM (Rapid Radiative Transfer Model) long-wave radiation scheme (Mlawer *et al* 1997), the Goddard short-wave radiation scheme (Chou and Suarez, 1994), the YSU (Yonsei University) planetary boundary layer scheme (Hong *et al* 2006), the Revised MM5 (fifth-generation Mesoscale Model) Monin-Obukhov surface layer scheme, and the Unified Noah land-surface model (Chen and Dudhia, 2001). A single-layer Urban Canopy Model is used to explicitly simulate the urban areas (Kusaka *et al* 2001). We have further updated the model land use types with the 2015 Terra and Aqua combined MODIS (Moderate Resolution Imaging Spectroradiometer) Land Cover Type (MCD12Q1) Version 6 data product.

We use the anthropogenic emissions from the 2015 Multi-resolution Emission Inventory for China (MEIC, http://www.meicmodel.org/) and 2010 MIX inventory for regions outside China (Li *et al* 2017), except for Chinese agricultural NH_3 emissions that are from Zhang *et al* (2018) with updated statistics for the year 2015. Biogenic emissions are calculated online using the Model of Emissions of Gases and Aerosols from Nature (MEGAN; Guenther *et al* 2006). Biomass burning emissions use Fire Inventory from the NCAR (FINN; Wiedinmyer *et al* 2011). Figure S2 shows the spatial distribution of NH_3, SO_2 and NO_x emissions over North China for January and July 2015, and Table S1 summarizes the emission totals. Our estimates of anthropogenic NH_3 emissions in North China are 0.11 Tg $month^{-1}$ in January and 0.25 Tg $month^{-1}$ in July. Compared with the MEIC NH_3 emissions, our estimates are about 1% lower in January and 44% higher in July.

We conduct a series of WRF-Chem simulations as summarized in Table 1. First, the baseline simulation (Base, corresponding to the S1R0 scenario) includes the emissions described above and can be evaluated with observations. Second, a group of sensitivity simulations (S1R*N*) by reducing anthropogenic NH_3 emissions over North China (110°-120°E and 35°-43°N; Figure S1) by 20%, 40%, 60%, 80%, and 100%, respectively (denoted as S1R*N* scenarios, *N* = 20/40/60/100). The differences in $PM_{2.5}$ concentrations between S1R0 and S1R*N* then estimate the effects of NH_3 emission reductions. Third, a group of sensitivity simulations (S2R*N*, *N* = 0/20/40/60/100), similar to S1R*N*, but further reduces the North China anthropogenic SO_2 emissions by ~40% and anthropogenic NO_x emissions by ~8% to reflect emission changes from 2015 to 2017 (Zheng *et al* 2018; Figure S3). Fourth, another group of sensitivity simulations, similar to S2R*N*, but further reduces anthropogenic NO_x emissions in North China by 20% (S3R*N*, *N* = 0/20/40/60/100). For all

simulations, a winter month (January) and a summer month (July) are simulated after 3-day spin-up for initialization.

For model evaluation, meteorological observations including 10-m wind direction (WD10), 10-m wind speed (WS10), 2-m air temperature (T2), and 2-m relative humidity (RH2) in January and July 2015 at 36 stations in North China are collected from National Climatic Data Center (NCDC, https://ncdc.noaa.gov/isd/data-access). Hourly observations of surface $PM_{2.5}$ concentrations at 39 stations in North China are obtained from the Ministry of Ecology and Environment (MEE) of China (http://106.37.208.233:2035/).

Monthly NH_3 concentrations at seven sites from the Ammonia Monitoring Network in China (AMoN-China; Pan *et al* 2018) are used to evaluate our NH_3 emission inventory in North China. We use NH_3 measurements from AMoN-China conducted during 01-31 January and 15-31 July 2015. We also use measurements of $PM_{2.5}$ components, including sulfate, nitrate, ammonium, organic carbon (OC) and black carbon (BC) in January and July 2015 at Beijing (39.94°N, 116.38°E) and Tianjin (39.09°N, 117.31°E) as obtained by the Institute of Atmospheric Physics (IAP). Hourly model simulated results are sampled at the grids covering the station locations. Correlation coefficient (*R*) and mean bias (MB) between observations and simulations are calculated.

3. *Observed and simulated surface pollutant concentrations*

Evaluations of model simulated meteorological variables (WD10, WS10, T2, and RH2) are shown in Figure S4. Simulated spatial patterns of meteorological variables are overall in good agreement with observations except for WD10 for which the model results are biased low in North China.

Figure 1 shows the time series and spatial distributions of observed and Base simulated $PM_{2.5}$ concentrations over North China in January (Figure 1a-b) and July (Figure 1c-d) 2015. The comparisons of $PM_{2.5}$ components with measurements at Beijing and Tianjin are shown in Figure S5. We find that the WRF-Chem Base simulation in general captures the magnitudes and variations of observed surface $PM_{2.5}$ concentrations in both January and July with correlation coefficients of 0.60-0.85 in January and 0.33-0.66 in July. The MB is small (2.6 μg m^{-3}) in January and relatively large in July (-9.1 μg m^{-3}). Evaluations with measurements of $PM_{2.5}$ components show that the model simulated SIA concentrations are biased low by 10-40% in July, likely suggesting the implemented heterogeneous sulfate formation (Chen *et al* 2016) still needs to be enhanced in summer.

We compare in Figure 2 the spatial distributions of measured and simulated surface NH_3 concentrations over North China for 01-31 January (Figure 2a) and 15-31 July (Figure 2c) 2015. Although measured and Base simulated NH_3 concentrations show similar spatial variations (*R* values of 0.93 in January and 0.72 in July), the Base model results are biased high by 38% (simulated 11.6 μg m^{-3} vs. observed 8.4 μg m^{-3}) in January and biased low by 30% (15.2 μg m^{-3} vs. 21.5 μg m^{-3}) in July. We find that when we decrease/increase anthropogenic NH_3 emissions by 20% in January/July, the biases can be nearly corrected in January and reduced to only -12% in July (Figure 2b and 2d). This indicates that our Base NH_3 emissions might be overestimated in January and underestimated in July over North China.

To further illustrate the effect of NH_3 emission changes on surface concentrations, we also show in Figure 2 changes in BTH regional mean gaseous NH_3, aerosol ammonium (NH_4^+), and total reduced nitrogen ($NH_x = NH_3+NH_4^+$) as we gradually reduce anthropogenic NH_3 emissions in North China (i.e., S1R*N* scenarios). When we begin to decrease NH_3 emissions (reductions < 40%), surface NH_3 concentrations decrease rapidly, while NH_4^+ concentrations decrease much slower, reflecting saturated NH_3 conditions with current emissions in particular for the January month. Under large emission reductions (> 60%), changes in aerosol NH_4^+ concentrations become faster than gaseous

NH_3 concentrations. Changes in the two species balance each other, leading a close-to-linear response of the NH_x concentrations to NH_3 emission reductions in North China. This is consistent with previous studies that suggest atmospheric NH_x is a better indicator of NH_3 emissions than NH_3 or NH_4^+ alone in the US (Pinder *et al* 2006; Zhang *et al* 2012).

4. Response of $PM_{2.5}$ pollution to NH_3 emission reductions

The sensitivity simulations with perturbed NH_3 emissions allow us to assess the responses of air pollution to NH_3 emission reductions. Figure 3 shows changes in surface $PM_{2.5}$ concentrations as we gradually reducing NH_3 emissions in North China in January 2015. To describe the saturation of atmospheric NH_3, we follow previous studies (Song *et al* 2018; Xu *et al* 2019) and define the excess NH_3 (in unit of μg m^{-3}) as the differences in NH_x and required NH_3 to meet ionic equilibrium using the formula below:

$$\text{Excess } NH_3 = \text{Total NHx} - \text{requred } NH_3 \quad (1)$$

$$\text{Total NHx} = 17 \times \left(\frac{[NH_4^+]}{18} + \frac{[NH_3]}{22.4}\right) \quad (2)$$

$$\text{requred } NH_3 = 17 \times \left(\frac{[SO_4^{2-}]}{48} + \frac{[NO_3^-]}{62} + \frac{[Cl^-]}{35.5} + \frac{[HNO_3]}{22.4} + \frac{[HCl]}{22.4} - \frac{[Na^+]}{23}\right) \quad (3)$$

where $[NH_4^+]$, $[SO_4^{2-}]$, $[NO_3^-]$, $[Cl^-]$, and $[Na^+]$ are the mass concentrations (in unit of μg m^{-3}) of these ions, and $[NH_3]$, $[HNO_3]$, and [HCl] are gas mixing ratios (ppb).

As shown in Figure 3, changes in the January mean $PM_{2.5}$ concentration become much more distinct with stronger NH_3 emission reductions in North China. The first 20% NH_3 emission reduction would only decrease $PM_{2.5}$ in Beijing by 1.6 μg m^{-3} and by 1.4 μg m^{-3} in BTH. The values increase to 8.3 μg m^{-3} in Beijing and 7.0 μg m^{-3} in BTH with 60% NH_3 emission reductions, and 20.8 μg m^{-3} in Beijing and 20.4 μg m^{-3} in BTH when all NH_3 emissions are turned off. The largest $PM_{2.5}$ responses shift towards the southern Hebei province where $PM_{2.5}$ concentrations are particularly high (Figure 1a). Such nonlinear responses can be largely explained by the derived excess NH_3 concentrations in each scenario. As also shown in Figure 3, NH_3 is highly saturated in the southern Hebei province in the Base condition and scenarios with small NH_3 emission reductions, and thus the SIA portion of $PM_{2.5}$ are insensitive to NH_3 emissions. We find similar results for July but with lower $PM_{2.5}$ decreases under strong NH_3 emission reductions than those in January (Figure S6).

Figure 4 summarizes the changes in BTH mean $PM_{2.5}$ and its components as driven by NH_3 emission changes in North China for January and July 2015. The decreases of $PM_{2.5}$ concentration associated with NH_3 emission reductions follow a power exponential function in January leading to small $PM_{2.5}$ changes under small NH_3 emission reductions. The responses in July are closer to a linear function. BTH mean $PM_{2.5}$ in July would be decreased by 1.6/5.3/11.1 μg m^{-3} with 20%/60%/100% NH_3 emission reductions in North China. The $PM_{2.5}$ components in both months show that aerosol sulfate has minor changes and aerosol nitrate can be substantially decreased with reducing NH_3 emissions, as also pointed out by Han *et al* (2020). We find stronger $PM_{2.5}$ responses in heavy pollution episodes in both months. As shown in Figure 4, for the highest 5% $PM_{2.5}$ concentrations, their values can be decreased by 4.5/24.2/64.4 μg m^{-3} when NH_3 emissions in North China are reduced by 20%/60%/100% in January. By contrast, the cleanest 5% $PM_{2.5}$ concentrations have nearly no change associated with NH_3 emission reductions.

Figure 4 also shows the responses of population-weighted $PM_{2.5}$ concentration (PWC) in North China as a metric more relevant to human health using population data from the Gridded Population of the World Version 4 (GPWv4) dataset (CIESIN 2018). PWC values show similar but larger responses than the regional geometric means. When NH_3 emissions in North China are reduced by 20-40%, monthly mean BTH PWC could be reduced by 1.4-3.8 μg m^{-3} (1.1-2.9% of PWC) in January and 1.8-3.6 μg m^{-3} (4.3-8.7% of PWC) in July. When NH_3 emissions are reduced by 60-100%, BTH PWC would be reduced by 8.1-26.7 μg m^{-3} (6.2-20.5% of PWC) in January and 5.9-

13.2 μg m^{-3} (14.4-32.0% of PWC) in July, illustrating $PM_{2.5}$ air quality improvements we can achieve by the NH_3 emission controls under 2015 emission conditions.
The analyses above have emphasized strong nonlinear responses of $PM_{2.5}$ concentrations to NH_3 emission changes in North China. To better quantify their effectiveness, we further calculate the NH_3 emission control efficiency based on the sensitivity simulations as $\beta_1 = \frac{\Delta PWC}{PWC} / \frac{\Delta E}{E}$, where $\frac{\Delta PWC}{PWC}$ is the relative change of PWC and $\frac{\Delta E}{E}$ is the relative change of NH_3 emissions in North China, denoting the relative response of PWC in percentage to 1% reduction in NH_3 emissions under each NH_3 emission scenario. We also calculate the absolute efficiency $\beta_2 = \Delta PWC / \Delta E$, describing changes in $PM_{2.5}$ per unit mass change in NH_3 emissions as shown in Figure S7. We find for the 2015 emission condition, the BTH mean β_1 efficiencies in January increase from 0.055 %/% in the Base condition to 0.48 %/% (a factor of 8.7 higher) when NH_3 emissions are reduced by 80%. The calculated β_1 efficiencies in July also indicate a nonlinear response, yet much weaker than January, with values of 0.22 %/% for the Base condition and 200% higher (0.65 %/%) when NH_3 emissions are 80% lower.

5. *Effects of NO_x and SO_2 emission changes*

We now quantify the influence of NO_x and SO_2 emission reductions on NH_3 emissions control efficiency. This can be estimated by comparing the S1R*N* with S2R*N* and S3R*N* scenarios. As described above, S1R*N* scenarios reflect NH_3 emission reductions for the 2015 emission condition, S2R*N* scenarios reflect the 2017 condition, and S3R*N* scenarios further consider 20% NO_x emission reduction. The differences of S2R0 minus Base and S3R0 minus S2R0 then estimate, respectively, the impacts of 2015-2017 SO_2/NO_x emission changes and further 20% NO_x emission reductions. The 2015-2017 emission changes (~40% reduction in SO_2 emissions and ~8% reduction in NO_x emissions) have led to decreases in BTH PWC $PM_{2.5}$ in both months (2.7 μg m^{-3} in January and 4.0 μg m^{-3} in July), mainly driven by the SO_2 emission reductions (Figure S8). With further 20% NO_x emission reductions, the BTH PWC would decrease by 1.9 μg m^{-3} in July, but increase by 1.0 μg m^{-3} in January (Figure S8). Reducing North China NO_x emissions alone in winter would increase ozone levels due to decreases in its titration and further enhance the formation of secondary aerosols, as recently found during the COVID-19 pandemic (Huang *et al* 2020).
Figure 5 shows the changes in BTH PWC and β_1 efficiency of NH_3 emission reduction in the S1R*N*, S2R*N*, and S3R*N* scenarios for January and July. We can see that the effects of 2015-2017 SO_2/NO_x emission reductions on BTH PWC improvements (4.6 in January and 4.9 in July) are comparable to 40-60% NH_3 emission reduction in 2015. The maximum BTH PWC reductions as can be achieved by NH_3 emission controls are 26.7 μg m^{-3} in January and 13.2 μg m^{-3} in July for the S1R*N* scenarios, and 27.6 μg m^{-3} in January and 9.4 μg m^{-3} in July for the S3R*N* scenarios. The much larger changes in July (13.2 vs. 9.4 μg m^{-3}) than January are mainly driven by the different responses of $PM_{2.5}$ to the 20% NO_x emission reduction. We can see that the impacts of the further 20% emission reduction on BTH PWC (as contributed by decreases in aerosol nitrate due to the NO_x emission reduction) in July become smaller with decreasing NH_3 emissions.
Changes in SO_2 and NO_x emissions can thus affect the efficiency of NH_3 emission reduction on $PM_{2.5}$ pollution. As shown in Figure 5, the 2015-2017 emission changes have generally decreased β_1 efficiencies, for no NH_3 emission reduction scenarios, from 0.055 %/% to 0.038 %/% (30% reduction) in January and from 0.22 %/% to 0.19 %/% (14% reduction) in July. SO_2 emission controls generally decrease the formation of ammonium sulfate aerosol, causing NH_3 in the air being saturated and thus suppressing the effectiveness of NH_3 emission controls. The additional 20% NO_x emission reduction would further suppress β_1 efficiencies in July but increase them in January, reflecting the enhanced nitrate formation due to NO_x emission reduction in BTH winter as

discussed above. Our results indicate that NH_3 emission controls at an earlier stage will be more effective for $PM_{2.5}$ air pollution regulation, and a joint NO_x and NH_3 emission control in winter will be more effective than controlling NO_x alone.

6. *Conclusions*

In summary, we have shown strong nonlinear responses of $PM_{2.5}$ air pollution to NH_3 emission reductions in North China. Using three sets of model simulations testing NH_3 emission reductions under different SO_2/NO_x emission conditions, we find that under the current NH_3 emission condition changes in $PM_{2.5}$ concentrations in North China associated with NH_3 emission reductions follow a power exponential function in January. The BTH January monthly mean PWC $PM_{2.5}$ concentrations would only decrease 1.4-3.8 μg m^{-3} (1.1-2.9% of $PM_{2.5}$) when NH_3 emissions in North China were reduced by 20-40%, but the decreases would reach 8.1-26.7 μg m^{-3} (6.2-20.5% of $PM_{2.5}$) with 60-100% NH_3 emission reductions. Such nonlinearity reflects a switch of NH_3-saturated to NH_3-limited condition for SIA, in particular, aerosol nitrate formation. The $PM_{2.5}$ changes in July also show a nonlinear response, but the nonlinearity is much weaker than January. As SO_2 emissions in North China have substantially reduced over 2015-2017, we find that has lowered the efficiency of NH_3 emission controls on $PM_{2.5}$ air pollution in both winter and summer. Future reductions of NO_x emissions may partly enhance $PM_{2.5}$ pollution in BTH winter due to the weakened titration effect, and can be offset by jointly controlling NH_3 emissions. Our results emphasize the importance of an accurate NH_3 emission estimate on the assessment of effectiveness of NH_3 emission controls, and also support the need to jointly consider emission reductions of SO_2, NO_x, and NH_3 for mitigating SIA air pollution.

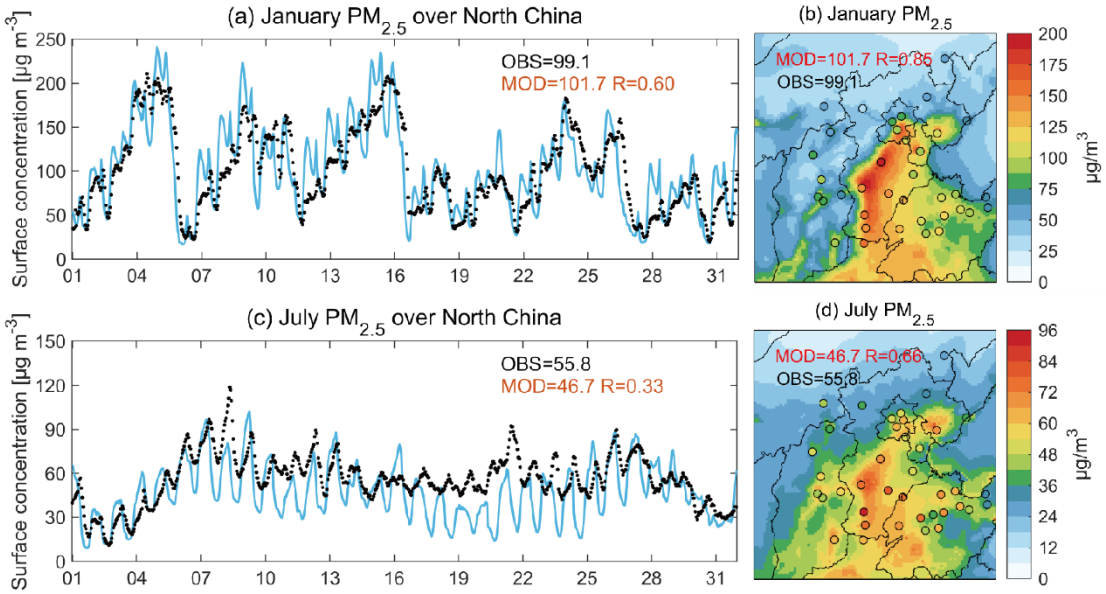

Figure 1. Observed and WRF-Chem Base simulated surface $PM_{2.5}$ concentrations over North China in January and July 2015. The left panels show time series of hourly observations (black dots) and model results (blue lines) by averaging 39 stations in North China. The right panels show space distributions of observed (circles) and simulated (contours) monthly mean concentrations. Regional monthly mean observed values (OBS) and corresponding model results (MOD), and their correlation coefficients (temporally and spatially) are shown inset.

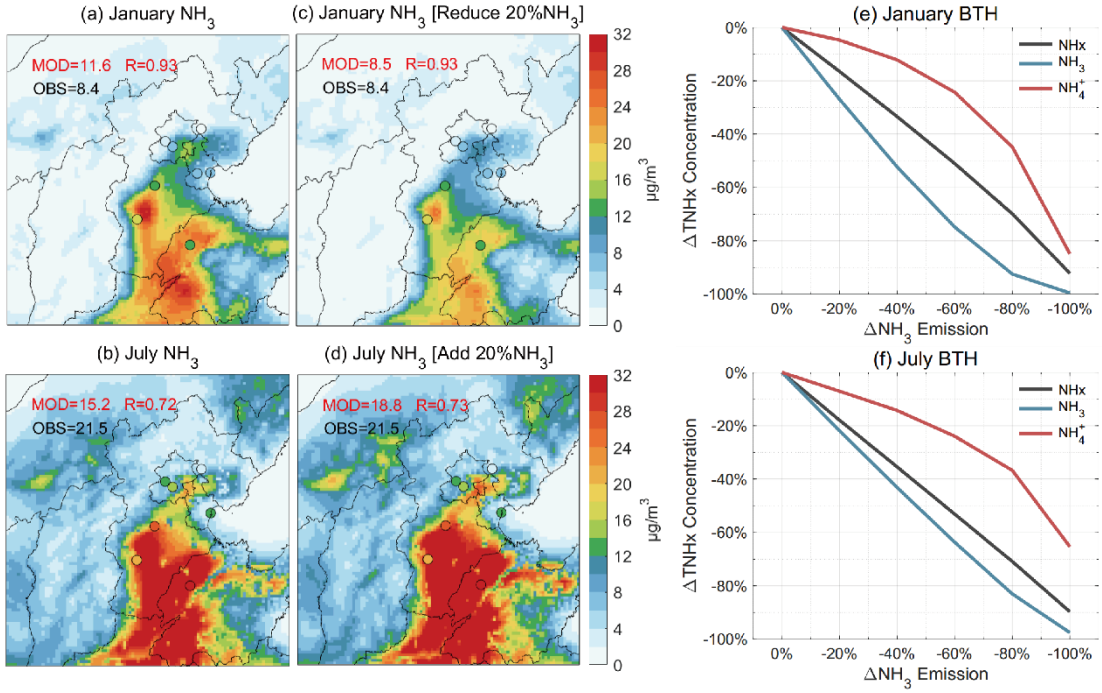

Figure 2. Observed and simulated surface NH_3 concentrations in North China for the periods of 01-31 January (top panels) and 15-31 July (bottom panels) 2015. The left panels show comparison of measurements (circles) with the Base simulation, and central panels show comparisons with sensitivity simulations (with NH_3 emissions in North China reduced by 20% for January and increased by 20% for July). Regional mean observed values (OBS) and corresponding model results (MOD), and their correlation coefficients are shown inset. The right panels show changes in Beijing-Tianjin-Hebei (BTH) mean gaseous NH_3 (blue lines), aerosol ammonium (NH_4^+, red lines), and total reduced nitrogen ($NH_x = NH_3+NH_4^+$, black lines) when NH_3 emissions in North China are decreased for January and July 2015.

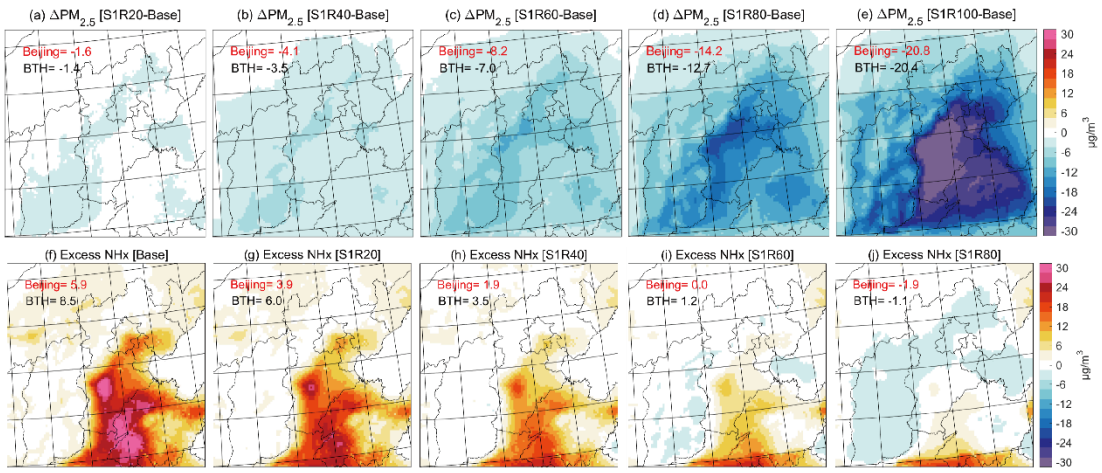

Figure 3. (Top panels) January mean changes in surface $PM_{2.5}$ concentrations due to NH_3 emission reductions in North China estimated as the differences between the Base simulation and S1R*N* scenarios with NH_3 emissions reduced by *N*% (*N* = 20/40/60/80/100). (Bottom panels) Excess NH_3 concentrations in January as estimated by the formula described in the text for the Base simulation and S1R*N* scenarios (*N* = 20/40/60/80). Regional mean values in Beijing and in BTH are shown inset.

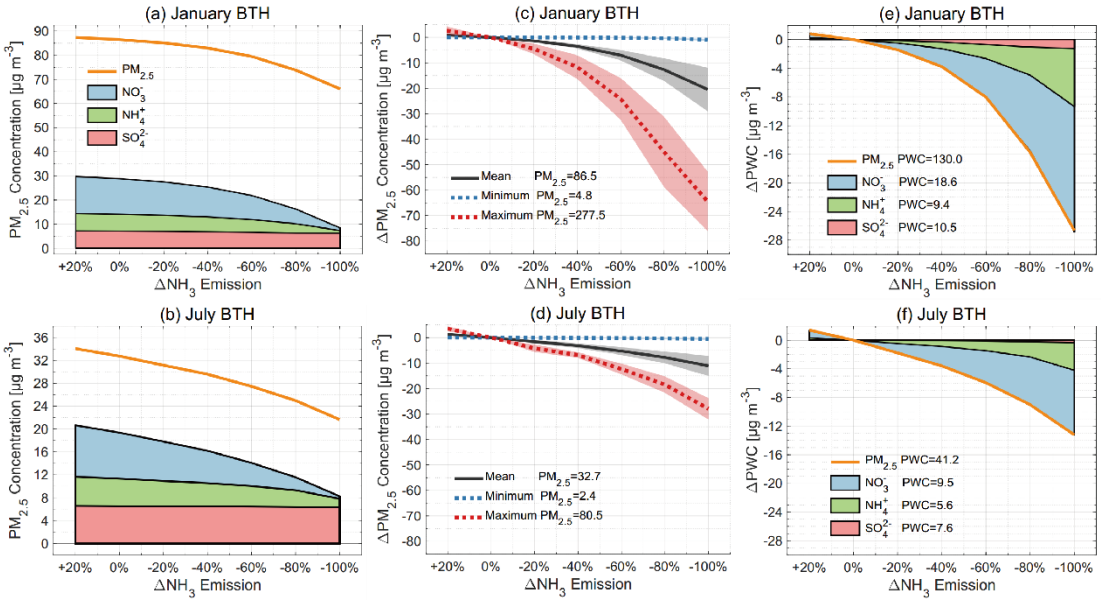

Figure 4. Effectiveness of NH_3 emission reductions in North China on BTH regional mean surface $PM_{2.5}$ pollution in January (top panels) and July (bottom panels) 2015. The left panels show BTH geometric mean $PM_{2.5}$ (orange lines), sulfate (red shading), ammonium (green shading), and nitrate (blue shading) levels. The central panels show reductions in monthly mean (black lines), minimum (blue dashed lines), and maximum (red dashed lines) $PM_{2.5}$ concentrations. The right panels show changes in population-weighted $PM_{2.5}$ (PWC) together with sulfate, ammonium, and nitrate contributions. Numbers inset are their values (ug m^{-3}) in the Base simulation.

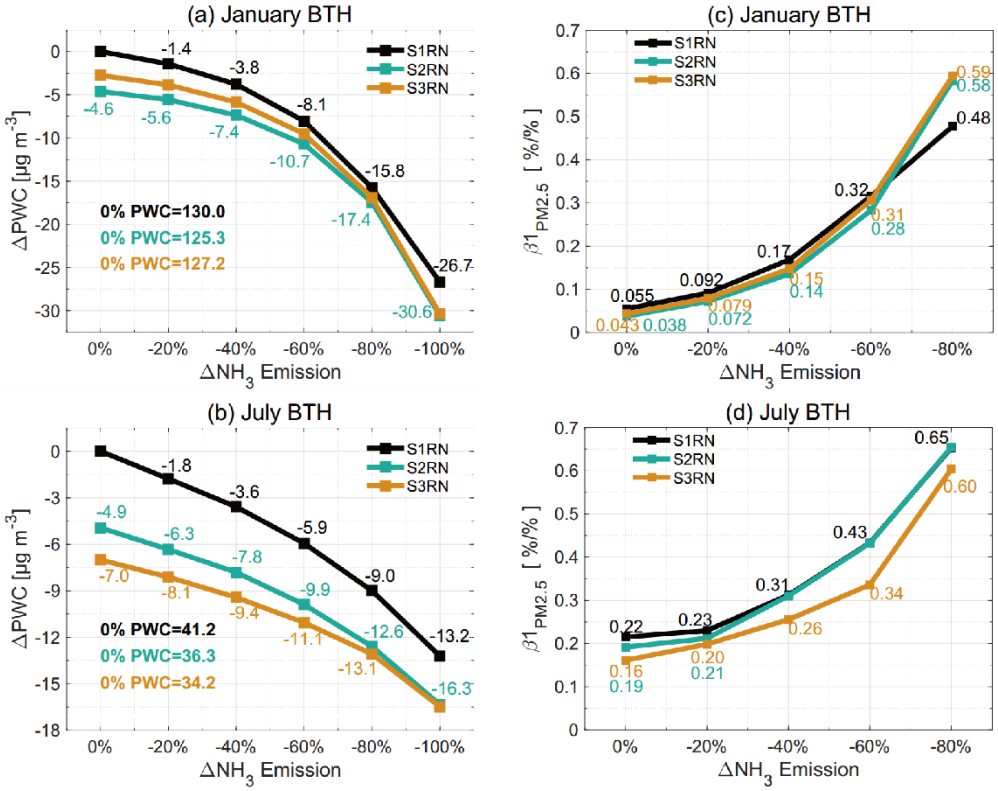

Figure 5. Changes in BTH PWC (left panels) and NH_3 emission reduction efficiency (right panels) in the S1R*N* scenarios (black lines; the 2015 emission condition), S2R*N* scenarios (green lines; the 2017 emission condition), and S3R*N* scenarios (orange lines, the 2017 emission condition with NO_x emission further reduced by 20%) in January (top panels) and July (bottom panels). BTH PWC

changes are relative to the Base simulated results (i.e., S1R0). PWC values for S1R0, S2R0, and S3R0 are given inset.

Table 1. Emission settings in the WRF-Chem simulation scenarios.

Simulation scenario	Description
Base	The 2015 emission conditions, also referred as S1R0
S1R*N* (*N* = 20/40/60/100)	NH_3 emission is reduced by 20%, 40%, 60%, 80% and 100%, respectively.
S2R*N* (*N* = 0/20/40/60/100)	Similar to S1R*N*, but further reduces the NO_x and SO_2 emissions from the levels of 2015 to those of 2017 in North China.
S3R*N* (*N* = 0/20/40/60/100)	Similar to S2R*N*, but further reduces NO_x emissions by 20% in North China.

References

Chen D *et al* 2016 Simulations of sulfate–nitrate–ammonium (SNA) aerosols during the extreme haze events over northern China in October 2014 *Atmos. Chem. Phys.* **16** 10707-24

Chen F *et al* 2001 Coupling an advanced land surface–hydrology model with the Penn State–NCAR MM5 modeling system. Part I: Model implementation and sensitivity *Mon. Weather Rev.* **129** 569-85

Center for International Earth Science Information Network (CIESIN) Columbia University 2018 Gridded Population of the World, Version 4 (GPWv4): Population Count, Revision 11 edited NASA Socioeconomic Data and Applications Center (SEDAC) Palisades, NY

Chou M D *et al* 1994 An Efficient Thermal Infrared Radiation Parameterization for Use in General Circulations Models *NASA Tech. Memo.* **104606** 3 p 85

Emmons L K *et al* 2010 Description and evaluation of the Model for Ozone and Related chemical Tracers, version 4 (MOZART-4) *Geosci. Model Dev.* **3** 43-67

Fu X *et al* 2017 Increasing Ammonia Concentrations Reduce the Effectiveness of Particle Pollution Control Achieved via SO_2 and NO_X Emissions Reduction in East China *Environ. Sci. Technol. Lett.* **4** 221-7

Gao J *et al* 2017 Haze, public health and mitigation measures in China: A review of the current evidence for further policy response *Sci. Total Environ.* **578** 148-57

Ge B *et al* 2019 Role of Ammonia on the Feedback Between AWC and Inorganic Aerosol Formation During Heavy Pollution in the North China Plain *Earth. Space. Sci.* **6** 1675-93

Grell G A *et al* 2002 A generalized approach to parameterizing convection combining ensemble and data assimilation techniques *Geophys. Res. Lett.* **29** 38-1--4

Guenther A *et al* 2006 Estimates of global terrestrial isoprene emissions using MEGAN (model of emissions of gases and aerosols from nature) *Atmos. Chem. Phys.* **6** 3181-210

Guo H *et al* 2018 Effectiveness of ammonia reduction on control of fine particle nitrate *Atmos. Chem. Phys.* **18** 12241-56

Han X *et al* 2020 Numerical analysis of agricultural emissions impacts on PM2.5 in China using a high-resolution ammonia emission inventory *Atmos. Chem. Phys.* **20** 9979-96

Hong S-Y *et al* 2006 A new vertical diffusion package with an explicit treatment of entrainment processes *Glob. Mon. Weather Rev.* **134** 2318-41

Huang X *et al* 2020 Enhanced secondary pollution offset reduction of primary emissions during COVID-19 lockdown in China *Natl. Sci. Rev.*

Huang R J *et al* 2014 High secondary aerosol contribution to particulate pollution during haze events in China *Nature* **514** 218-22
Kusaka H *et al* 2001 A simple single-layer urban canopy model for atmospheric models: Comparison with multi-layer and slab models *Bound. - Layer Meteor.* **101** 329-58
Li M *et al* 2014 Haze in China: current and future challenges *Environ. Pollut.* **189** 85-6
Li M *et al* 2017 MIX: a mosaic Asian anthropogenic emission inventory under the international collaboration framework of the MICS-Asia and HTAP *Atmos. Chem. Phys.* **17** 935-63
Ministry of Ecology and Environment of the People's Republic of China (MEE), 2016 *Report on the State of the Environment in China 2013* http://english.mee.gov.cn/Resources/Reports/soe/soe2011/201606/P020160601591756378883.pdf. Accessed 29 September 2020.
Ministry of Ecology and Environment of the People's Republic of China (MEE), 2018 *Report on the State of the Ecology and Environment in China 2017* http://english.mee.gov.cn/Resources/Reports/soe/SOEE2017/201808/P020180801597738742758.pdf. Accessed 29 September 2020.
Mlawer E J *et al* 1997 Radiative transfer for inhomogeneous atmospheres: RRTM, a validated correlated-k model for the longwave *J. Geophys. Res.-Atmos.* **102** 16663-82
Pan Y *et al* 2018 Identifying Ammonia Hotspots in China Using a National Observation Network *Environ. Sci. Technol.* **52** 3926-34
Pinder R W *et al* 2006 Temporally resolved ammonia emission inventories: Current estimates, evaluation tools, and measurement needs *J. Geophys. Res.-Atmos.* **111**
Seinfeld J H and Pandis S N 2006 *Atmospheric Chemistry and Physics: From Air Pollution to Climate Change* (New York: Wiley)
Song S *et al* 2018 Fine-particle pH for Beijing winter haze as inferred from different thermodynamic equilibrium models *Atmos. Chem. Phys.* **18** 7423-38
Song S *et al* 2019 Thermodynamic Modeling Suggests Declines in Water Uptake and Acidity of Inorganic Aerosols in Beijing Winter Haze Events during 2014/2015–2018/2019 *Environ. Sci. Technol. Lett.* **6** 752-60
State Council of the People's Republic of China (SC), 2013 *Notice of the State Council on Issuing the Action Plan on Prevention and Control of Air Pollution* http://www.gov.cn/zhengce/content/2013-09/13/content_4561.htm. Accessed 29 September 2020.
State Council of the People's Republic of China (SC), 2018 *Notice of the State Council on Issuing the Three-year Action Plan Fighting for a Blue Sky* http://www.gov.cn/zhengce/content/2018-07/03/content_5303158.htm. Accessed 29 September 2020.
Sun Y *et al* 2012 Characterization of summer organic and inorganic aerosols in Beijing, China with an Aerosol Chemical Speciation Monitor *Atmos. Environ.* **51** 250-9
Sun Y *et al* 2016 Rapid formation and evolution of an extreme haze episode in Northern China during winter 2015 *Sci. Rep.* **6** 27151
Thompson G *et al* 2009 Impact of Cloud Microphysics on the Development of Trailing Stratiform Precipitation in a Simulated Squall Line: Comparison of One- and Two-Moment Schemes *Mon. Weather Rev.* **137** 991-1007
Wang Y *et al* 2013 Sulfate-nitrate-ammonium aerosols over China: response to 2000–2015 emission changes of sulfur dioxide, nitrogen oxides, and ammonia *Atmos. Chem. Phys.* **13** 2635-52
Wiedinmyer C *et al* 2011 The Fire INventory from NCAR (FINN): A high resolution global model to estimate the emissions from open burning *Geosci. Model Dev.* **4** 625-41
Xu Z *et al* 2019 High efficiency of livestock ammonia emission controls in alleviating particulate nitrate during a severe winter haze episode in northern China *Atmos. Chem. Phys.* **19** 5605-13

Zaveri R A *et al* 1999 A new lumped structure photochemical mechanism for large-scale applications *J. Geophys. Res.-Atmos.* **104** 30387-415
Zaveri R A *et al* 2008 Model for Simulating Aerosol Interactions and Chemistry (MOSAIC) *J. Geophys. Res.* **113**
Zhang L *et al* 2012 Nitrogen deposition to the United States: distribution, sources, and processes *Atmos. Chem. Phys.* **12** 4539-54
Zhang L *et al* 2015 Source attribution of particulate matter pollution over North China with the adjoint method *Environ. Res. Lett.* **10** 084011
Zhang L *et al* 2018 Agricultural ammonia emissions in China: reconciling bottom-up and top-down estimates *Atmos. Chem. Phys.* **18** 339-55
Zhang Q *et al* 2019 Drivers of improved $PM_{2.5}$ air quality in China from 2013 to 2017 *Proc. Natl Acad. Sci. USA* **116** 24463-9
Zhao P S *et al* 2013 Characteristics of concentrations and chemical compositions for $PM_{2.5}$ in the region of Beijing, Tianjin, and Hebei, China *Atmos. Chem. Phys.* **13** 4631-44
Zheng B *et al* 2018 Trends in China's anthropogenic emissions since 2010 as the consequence of clean air actions *Atmos. Chem. Phys.* **18** 14095-111